Efficient evanescent coupling design for GeSi electro-absorption modulator

Li Ya-Ming(李亚明)† and Cheng Bu-Wen(成步文)

State Key Laboratory on Integrated Optoelectronics, Institute of Semiconductors, Chinese Academy of Sciences, Beijing 100083, *China*

(Received 12 March 2013; revised manuscript received 28 March 2013)

Efficient coupling from the silicon waveguide to the GeSi layer is the key to success in the GeSi electro-absorption (EA) modulator based on evanescent coupling. A lateral taper in the upper GeSi layer has room for increasing the modulating efficiency and alleviating the sensitivity of the extinction ratio (ER) and insertion loss (IL) to the length of the active region. The light behavior and the effect of the taper are explored in detail using the beam propagation method (BPM). After optimization, the light can nearly be totally confined in the GeSi layer without any oscillation. The modulator with the designed taper can achieve low IL and high ER.

Keywords: electro–optical modulators, waveguides, integrated optoelectronic circuit

PACS: 42.79.Hp, 42.82.–m, 78.66.–w **DOI:** 10.1088/1674-1056/22/12/124209

1. Introduction

Silicon photonics is pinned on a great hope: to bring revolution to the on-chip interconnects. As a critical component, the optical modulator on silicon has proved difficult to realize in practical devices, owing to the weak electro–optical effect of silicon.[1] However, in contrast, the electro-absorption (EA) effect does not rely on the carrier density change. EA modulators could potentially achieve a large bandwidth and a practical optical bandwidth with a low operating energy.[2–11] Currently, several silicon-based GeSi or Ge EA modulators adopting either butting coupling or evanescent coupling are being demonstrated.[12–17] In contrast to the butting coupling mechanism, an evanescent-coupled structure is more favorable. It can achieve a lower optical coupling loss between the bus waveguide and the active region. Moreover, the GeSi can be grown directly on the silicon-on-insulator (SOI) without selective epitaxy and the following CMP. The fabrication process is relatively simple. However, the reported evanescent-coupled Ge modulator[14] endures a large insertion loss (IL) of 9.6 dB. Moreover, most detectors adopting this evanescent coupling mechanism will have the problem of coupling efficiency. In this paper, we present a detailed discussion of the light behavior in the evanescent-coupled GeSi EA modulator using the beam propogation method (BPM). Because of the multiple modes in the active region, the light will oscillate between the SiGe layer and the Si waveguide. This oscillation will degrade the modulation performance. The active length must be equal to some special value where the light is precisely located at the Si waveguide for a low IL and a high extinction ratio (ER). This complicates the design. In this paper, we introduce a lateral taper in the GeSi layer. The sensitivities of the coupling efficiency, ER and IL to the device parameters, in principle, can be eliminated. This kind of taper can also be used in the evanescent coupling detectors with low absorption coefficients.

2. Light behavior and structure design

The three-dimensional (3D) schematic view and the cross section of the GeSi modulator are shown in Figs. 1(a) and 1(b), respectively. The GeSi layer can be grown directly on the top of the rib silicon waveguide to form a lateral p–i–n structure. The GeSi layer and the rib waveguide have the same width of w. To focus on coupling between the Si waveguide and the active region, we set the imaginary part of the refractive index to be zero. The semi-vector BPM is adopted to simulate the light propagation. Instead of using the directional coupling mode, we treat the modulator as a whole. The thickness of the top Si of SOI is 0.34 μm. The Si rib waveguide meets the single mode condition and the fundamental mode is shown in Fig. 2(a). We first investigate a modulator with $w = 0.4$ μm and $t_{\mathrm{GeSi}} = 0.2$ μm, which is similar to that in Ref. [4]. There are two guided modes in the active region, which are shown in

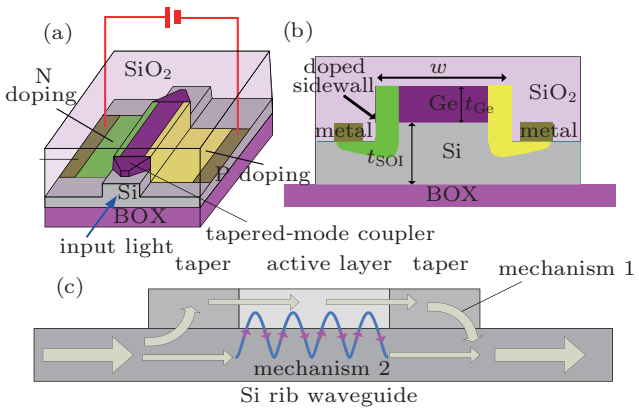


Fig. 1. (color online) (a) 3D schematically view and (b) cross-section view of the evanescent-coupled GeSi EA modulator structure; (c) the two coupling mechanisms in the proposed modulator.

†Corresponding author. E-mail: ymli@semi.ac.cn

© 2013 Chinese Physical Society and IOP Publishing Ltd

Figs. 2(b) and 2(c). The propagation constants are β_1 and β_2, which are 12.64 μm^{-1} and 2.57 μm^{-1}, respectively. For the modulator without the taper, the optical power coupling into the active region is distributed in the two modes of the active region.

The two modes will propagate coherently, leading to multi-mode interferences. The field profile at a distance z is given by

$$E = E_1 + E_2 = c_1 e_1(y) \exp[\mathrm{j}(wt - \beta_1 z)] + c_2 e_2(y) \exp[\mathrm{j}(wt - \beta_2 z)], \quad (1)$$

where c_1 and c_2 are the field excitation coefficients. Taking the phase of the fundamental mode as a common factor out of the sum, dropping it and assuming the time-dependent $\exp(\mathrm{j}wt)$ is implicit, then the field profile of the light in the active region can be written as follows:

$$E = c_1 e_1(y) + c_2 e_2(y) \exp[\mathrm{j}(\beta_1 - \beta_2) z]. \quad (2)$$

If

$$z = \frac{2n\pi}{\beta_1 - \beta_2} = 2.82\ \mu\mathrm{m},$$

the two modes will be in phase and the input field will therefore be repeated like a multimode interferometer (MMI), just as is shown in Fig. 2(g). That is to say, the light in the active region will oscillate back into the fundamental mode of the Si waveguide beneath the GeSi layer. The corresponding field profile is shown in Fig. 2(d). However, if the two modes are in antiphase, instead of the mirror images of the input field, the superposition of the two modes can be formed because of the structural asymmetry. The field profile is shown in Fig. 2(e). In the whole active region, the light will oscillate between the state of Fig. 2(d) and the state of Fig. 2(e). Correspondingly, there is only half of the active region that is effective. Moreover, the active length must be equal to some special value where the light is precisely coupled back into the fundamental mode of the Si waveguide for a low IL. Otherwise, the light will be scattered at the output and cannot be coupled into the bus waveguide in the state of the modulator, just as Fig. 2(f) shows. This may be the reason why there is a large IL in the modulator of Ref. [5].

As we can see in Figs. 2(b) and 2(c), the fundamental mode is almost confined in the GeSi layer, but the first mode leaks into the Si layer. If all the light can be coupled from the bus waveguide into the fundamental mode of the active region, then the oscillation can be eliminated. The effective modulating length will be lengthened. The active length could not be subjected to the oscillation. In this structure, we introduce a lateral taper to achieve the total mode transfer of the mode of the Si waveguide into the fundamental mode of the active region.

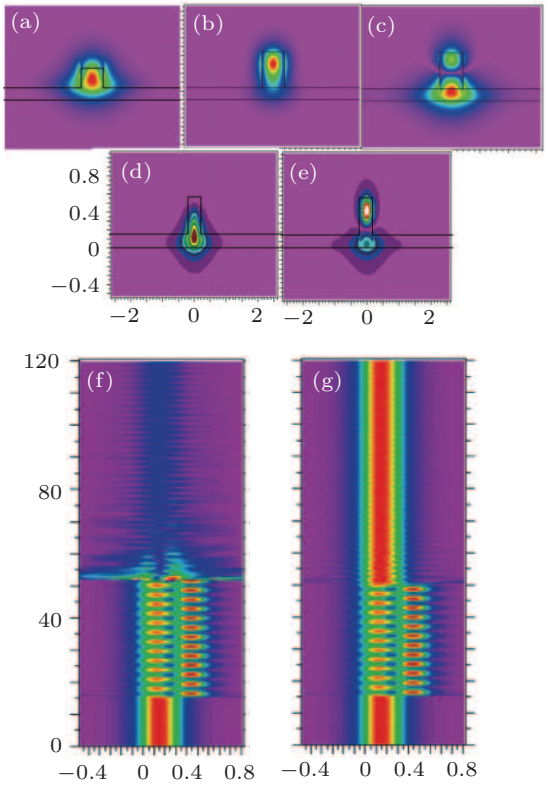


Fig. 2. (color online) (a) Fundamental mode of the Si waveguide in the GeSi region, (b) the second mode of the GeSi region; the mode profile when the two modes are in phase (d) and in antiphase (c); the light coupling into (f) does not couple into the bus waveguide.

Here, we introduce a balance factor f, which means the optical power in the fundamental mode of the active region needs to counteract the optical power in the second mode in the GeSi layer. If f is equal to zero, the light will be totally coupled into the fundamental mode of the active region. Formula (2) is equivalently rewritten as follows:

$$E = \underline{(1-f)\, c_1 e_1(y)} + \underline{\underline{\{f c_1 e_1(y) + c_2 e_2(y) \exp[\mathrm{j}(\beta_1 - \beta_2) z]\}}}.$$

Based on the formula given above, we can define two mechanisms for light to route through the active region, as shown in Fig. 1(c).

Mechanism I This mechanism corresponds to the first part of the formula with single underlining. This part of light is the partial power of the light in the fundamental mode of the active region. It will propagate independently without any oscillation and can be recovered at the end of the active region. This mechanism becomes dominant when more light is coupled into the fundamental mode of the active region.

Mechanism II Coherent propagation process. This mechanism corresponds to the second part of the formula with double underlining. This part of light includes the light in the second mode of the active region and partial light in the fundamental mode. It will propagate coherently along the active region with oscillation.

We can clearly come to the conclusion that because of the second mode of the active region, mechanism II is the reason for the oscillation and low modulating efficiency.

To investigate the behavior of light in the modulator, an initial calculation was made of nearly a 100 percent mode converter through the tapered-mode converter with a taper tip width of 0.15 μm and a taper length of 10 μm. Figure 3 shows the BPM-calculated results; the main coupling takes place within a length from 4 μm to 5.8 μm centered at the intersection of the effective index, which is situated at a coupling length of 4.9 μm. When the coupling length > 6 μm, nearly 100 percent of the light power is transferred into the fundamental mode of the GeSi layer. The BPM simulation results indicate that the lateral tapered-mode converter can achieve total mode transfer by proper design. The main transfer takes place within a length centered at the intersection of the effective index. The taper tip width should be small enough to make the propagation constant of the fundamental mode of the GeSi intersecting with that of Si. The converter length should be long enough to achieve total mode transfer. In the following text, we identify some critical value of the taper for total mode transfer.

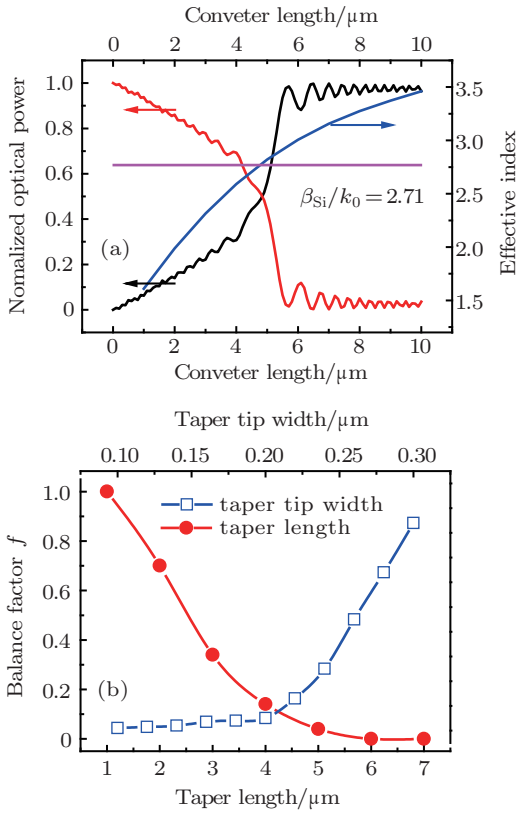


Fig. 3. (color online) (a) Strong mode transfer occurring when the effective index intersects; (b) the dependences of balance factor on taper length and taper tip width.

Figure 3(b) shows the dependences of balance factor f on the taper tip width when the taper length is long enough (10 μm). The factor f is determined to be the minima of the output power at different active lengths. At the minima, the light that is not coupled into the GeSi layer by the mechanism I is scattered at the end of the modulator because of the oscillation in mechanism II. In this case, the coupling mechanism I is the only one for the output power. That is to say, a smaller f means a large mode converter. As can be seen in Fig. 3(b), f nearly reaches zero when the taper tip width is smaller than 0.2 μm, which means that the intersection of the GeSi propagation coefficient with that of the Si waveguide occurs when $w > 0.2$ μm. It is necessary for the taper tip to be sharper to assure the intersection. In the practical application, we can set the taper tip width to be 0.15 μm and the fabrication tolerance can be at least 50 nm.

The line with circles in Fig. 3(b) shows the dependence of the balance factor f on the taper length. The tip width is set to be 0.15 μm. The f factor (0.05) nearly reaches zero when the taper length is larger than 5 μm. In this case, mechanism I is the dominant one for the light passing through the active region. The power in the silicon mode is nearly totally transferred into the fundamental mode of the active region.

To investigate the effect of GeSi thickness on the modulating efficiency, we set the absorption coefficient of the GeSi at the wavelength of 1.55 μm to be 633 cm^{-1} (the absorption coefficient of $Ge_{0.9925}Si_{0.0075}$ at 100 kV/cm can be found in Ref. [2]). The absorption power after a 50-μm-long active region with a 6-μm taper is calculated. The taper tip width is 0.15 μm. As Fig. 4 shows, when the GeSi thickness is larger than 0.2 μm, the absorbed power is saturated. Similarly, we calculate the absorption power after a 56-μm-long active length without a taper. The absorbed power oscillates with the GeSi thickness without saturation. The device parameters need to be designed carefully for maximum effect, which is treated as the coupling efficiency in Refs. [18] and [19]. In contrast, the modulator or detector with the taper will achieve and retain stable saturation after some thickness. This is another proof that the tapered-mode coupler enables the total mode transfer and increase the detecting or modulating efficiency.

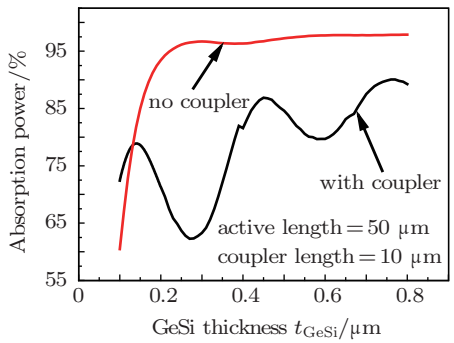


Fig. 4. (color online) Absorbed powers of the GeSi modulator at different GeSi thickness values.

With a series of designs of the taper, we make a comparison of the performance of the modulator between either with or without the taper mode converter. The taper length and taper tip width can be set to be 0.15 μm and 6 μm, respectively. The Si composition of the GeSi is set to be 0.75% with the absorption coefficients of 158/cm and 633/cm at 10 kV/cm and 100 kV/cm, respectively.[14]

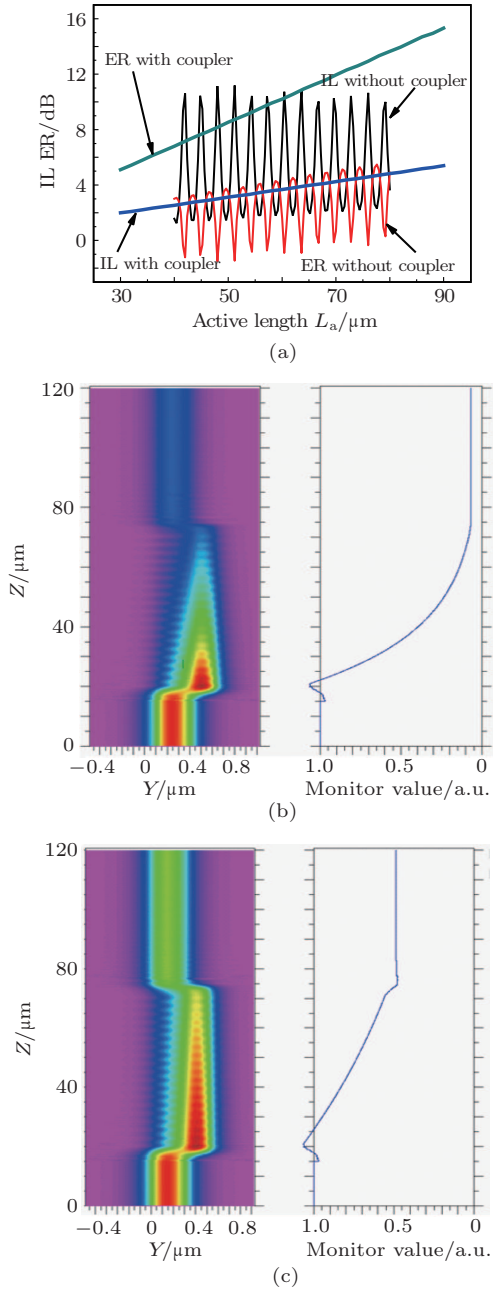


Fig. 5. (color online) (a) ER and IL versus device length for the modulator; (b) and (c) YZ plane view of light propagation in the modulator with 50-μm-long active length for (b) off state and (c) on state.

Figure 5(a) shows the plots of the ER and IL versus the active length at a wavelength of 1.55 μm. For a 50-μm-long modulator, we achieve an ER of 8.5 dB and a corresponding IL of 3.1 dB, i.e., 2.8-dB material absorption loss and 0.3-dB coupling loss introduced by the material absorption of the tapered coupler. As far as the modulator based on mechanism II is concerned, the ER and IL show sharp oscillation with the active length. The local maximum of ER and the corresponding minimum of the IL occur at the active length where the light is coupled into the Si waveguide, like the case in Fig. 2(b). If the light is not coupled into the Si waveguide at the output of the active region just as is shown in Fig. 2(b), the light will be scattered. There will be no power output in both the on state and the off state, which results in a very large IL and eliminates the modulating effect. Moreover, for the same 50-μm-long active length, mechanism I can remarkably enable a larger ER. Figures 5(b) and 5(c) show the off-state and on-state light propagation, respectively. The light is totally coupled into the GeSi modulating layer by the mechanism I without any oscillator. So just because of the nearly 100 percent mode transfer by the coupler, the IL and ER could increase linearly with the active length increasing. The active length needs no detailed design to be equal to some special value where the light is precisely coupled into the basic mode of the rib waveguide to be sure of a low IL and a high ER.

3. Conclusions

We investigated the light behavior in the GeSi EA modulator based on evanescent coupling. Instead of a directional coupling mode based on coupling mode theory, multimode interference and mode transfer can successfully describe our structure. We indentify two coupling mechanisms. The BPM simulation shows that the light will oscillate, owing to mechanism II. An inappropriate active length will lead to a large IL and eliminate the modulating effect. Mechanism I becomes dominant after the introduction of the taper mode converter. The modulator based on mechanism I shows a high ER, which is comparable to that of the butt-coupling GeSi modulator. Especially, the coupling loss is as low as 0.3 dB. This taper mode converter can be used in a similar bottom-to-top evanescent coupling structure.

References

[1] Reed G T, Mashanovich G, Gardes F Y and Thomson D J 2010 *Nat. Photon.* **4** 518
[2] Zhao L J, Chen W X and Wang W 2007 *Acta Phys. Sin.* **56** 2751 (in Chinese)
[3] Feng X Q, Chen F and Hou X 2003 *Acta Phys. Sin.* **52** 761 (in Chinese)
[4] She W L and Wu D D 2005 *Acta Phys. Sin.* **54** 134 (in Chinese)
[5] Zhao L J, Wang Y and Wang W 2010 *Chin. Phys. B* **19** 124215
[6] Xu K S, Sui Z and Ge A M 2003 *Acta Phys. Sin.* **52** 2481 (in Chinese)
[7] Wang W, Zhao L J and Zhu H L 2010 *Chin. Phys. B* **19** 074216
[8] Qin Z X, Cen L B and Shen B 2009 *Chin. Phys. B* **18** 3905
[9] Yang H, Wang W and Liao Z Y 2008 *Chin. Phys. B* **17** 2557
[10] Tu X G, Chen S W and Yu J Z 2006 *Physics* **35** 317 (in Chinese)
[11] Sun F and Yu J Z 2005 *Physics* **34** 50 (in Chinese)
[12] Liu J F, Pan D, Jongthammanurak S, Wada K, Kimerling L C and Michel J 2007 *Opt. Express* **15** 623
[13] Liu J F, Beals M, Pomerene A, Bernardis S, Sun R, Cheng J, Kimerling L C and Michel J 2008 *Nat. Photon.* **2** 433
[14] Lim A E J, Yang T L, Qing F, Duan N, Yu M B, Lo G Q and Kwong D L 2011 *Opt. Express* **6** 5040
[15] Feng N N, Feng D Z, Liao S R, Wang X, Dong P, Liang H, Kung C C, Qian W, Fong J, Shafiiha R, Luo Y, Cunningham J, Krishnamoorthy A V and Asghari M 2011 *Opt. Express* **19** 7062
[16] Feng D Z, Liao S R, Liang H, Fong J, Bijlani B, Shafiiha R, Luff B J, Luo Y, Cunninghan J, Krishnamoorthy A V and Asghari M 2012 *Opt. Express* **20** 22224
[17] Li Y M, Hu W H, Cheng B W, Liu Z and Wang Q M 2012 *Chin. Phys. Lett.* **29** 034205
[18] Ahn D H, Kimerling L C and Jurgen M 2010 *J. Light Technol.* **28** 3387
[19] Zhang Y, Kao T T, Liu Z, Lochner Z, Kim S S, Ryou J H, Dupuis R D and Shen S C 2011 *J. Appl. Phys.* **109** 083115